TEMPERATURE-DEPENDENT SPECTRAL OBSERVATIONS OF PYROXENE POWDERS. M. S. Shusterman[1], B. R. Wing[1], R. L. Klima[1], C. A. Hibbitts[1], and N. R. Izenberg[1]. [1]Johns Hopkins University Applied Physics Laboratory, Laurel, MD. (Contact Author: Mshusterman@ser.asu.edu).

Introduction: The 1-µm and 2-µm absorption features in pyroxenes are strongly affected by electronic transitions in ferrous iron and other transition elements [1]. However, the physical effects of temperature variations on transition element coordination sites also have significant impact on the width, depth, and position of spectral absorption features [1-7]. Singer and Roush [2] found that temperature affects the extent of M(2) site distortion, with increasing temperatures causing the site to become more distorted in orthopyroxenes distorted in clinopyroxenes. Thus, the changes to absorption features across a range of temperatures can be diagnostic of mineral composition and can provide information that aids the interpretation of remote sensing data [8].

Previous studies have investigated the relationship between temperature and spectral absorption features of pyroxenes and olivines, but the sample suite has been relatively limited. This study investigates how the absorption features of three pyroxenes (ortho and clino) with a range of iron weight percents are affected by temperature in the near-infrared wavelength range. To describe the spectral variations, we evaluated each mineral's thermospectrum, defined as the change in reflectance R with respect to temperature T as a function of wavelength. The thermospectrum gives the wavelength dependency of $\Delta R/\Delta T$ thereby providing a mechanism to refine a compositional analysis for remotely sensed spectral data, including transition element weight percent.

Methods: *Experimental Design:* Enstatite, diopside, and hedenbergite samples containing ~0.5%, ~2%, and ~17% iron oxide respectively, were hand ground and dry-sieved to <75 µm. Powders were lightly compacted into an aluminum sample plate containing a thermocouple then covered with a magnesium fluoride window to prevent grain escape into the vacuum system. The aluminum plate was mounted onto a copper fixture, adjacent to a gold standard, and then affixed to a vertical cryostat (Fig. 1). The stainless steel vacuum chamber was evacuated to high-vacuum pressures using a Pfeiffer HiPace 300 turbo pump backed by an Edwards nXDS15i dry scroll pump. A manipulator attached to the cryostat allowed for vertical movement of the sample plate while the chamber was evacuated, facilitating background measurements between each sample measurement. Illumination was provided by a halogen lamp with i=15˚ and e=45˚. Spectra in the NIR wavelength range were acquired using an InfraRed Associates ID313 liquid nitrogen cooled MCT detector, capable of collection from 0.7-16.0 µm. Each IR spectrum was the integration of 150 scans across wavelengths of 0.7-5.0 µm. Spectra were collected from room temperature down to cryogenic temperatures using liquid nitrogen, then heated to ~450K using a button heater mounted to the back of the copper fixture.

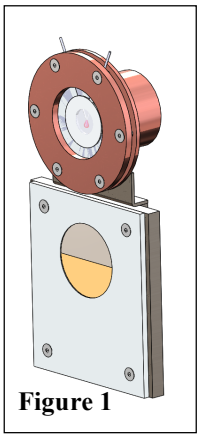
Figure 1

Analytical Methods: Thermal expansion and contraction of the sample holder and cryostat that resulted in mechanical shifts affected the spectrum in a wavelength independent manner and were removed from the spectra by normalizing the background measurements across the same range of temperatures at which samples were measured. A straight-line continuum was estimated for each spectrum by selecting maximum reflectance values at the short and long wavelength shoulders of each major absorption band. Band position, intensity, and width were evaluated from continuum-removed spectral plots that were generated by dividing spectra by their continua.

Results: *Enstatite (Fig. 2a):* The ~920 nm band depth did not change significantly as a function of temperature, though the band width increased on the long-wavelength shoulder as temperatures increased. As a result, the FWHM increased by 41 nm. The ~1825 nm band depth shallowed by 8% as temperatures increased by 320 K, accompanied by a 52 nm longward shift in band position and a 100 nm increase in FWHM. The thermospectrum (red in Fig. 3) shows a relatively constant relationship between $\Delta R/\Delta T$ and wavelength from 650-2600 nm, with slight negative peaks occurring at 1020 nm and 2130 nm.

Diopside (Fig. 2b): The ~1058 nm band position did not change significantly with increasing temperatures, but band depth shallowed by 4% and the FWHM increased by 104 nm over 355 K. The ~2325 nm band position shifted shortward by 12.5 nm and shallowed by 7% as temperatures increased. Sample contamination caused minor bands to appear within the 2325 nm feature, therefore a fit was used to determine band minima. The FWHM decreased by 124 nm across the same temperature range. The ~2325 nm band was the most sensitive wavelength range across the diopside spectra, with the long-wavelength shoulder having the highest sensitivity to temperature (Fig. 3).

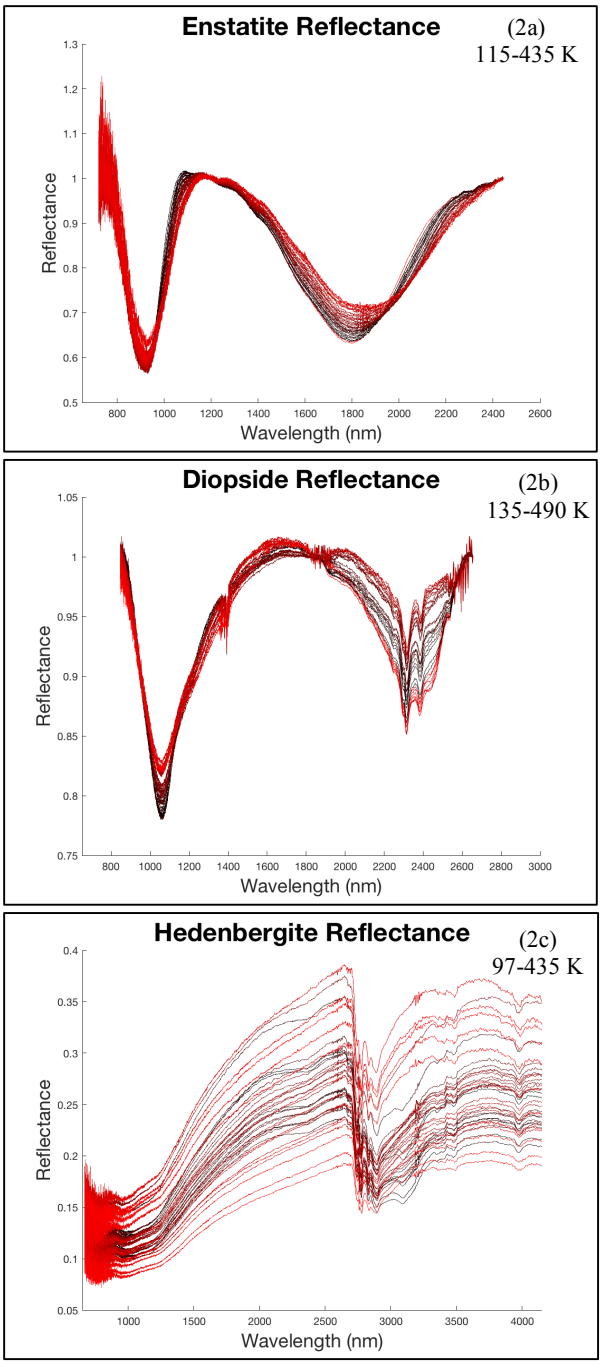

Figure 2. 2a,2b: Continuum-removed reflectance spectra of enstatite and diopside. 2c: Corrected reflectance spectra of hedenbergite. Hot spectra are red, cold spectra are black.

Hedenbergite (Fig. 2c): The band minima of the hedenbergite sample fell within the visible wavelength range; not covered in this dataset. A temperature dependency across the NIR range was still detectable, primarily in the broadening of the long-wavelength shoulder, across ~1250-2500 nm. The $\Delta R/\Delta T$ sensitivity increased slightly with increasing wavelength.

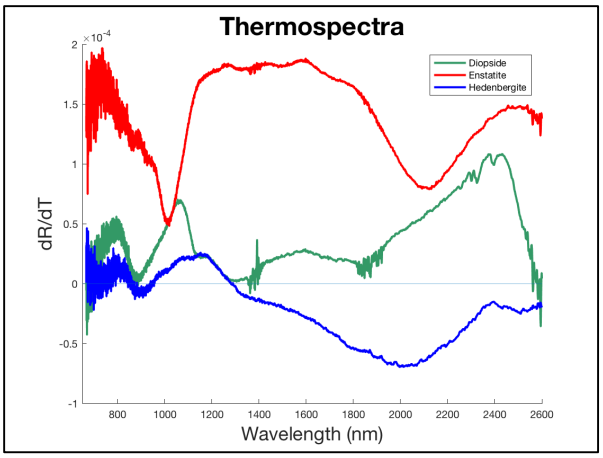

Figure 3. Thermospectra showing the relationship between reflectance and temperature with respect to wavelength of the three observed samples. The magnitude of divergence from zero indicates the sensitivity of the mineral's reflectance to temperature at a given wavelength.

Summary: All three minerals, with FeO abundances ranging from ~0.5% to ~17%, displayed varying amounts of spectral dependency on temperature. This study had findings consistent with data from [2] and [6], in which temperature variations primarily affected band symmetry at the long-wavelength edge. Previous studies have shown that band positions move to longer wavelengths with increasing iron and calcium abundances [5], and this study indicates that temperature variations may replicate the shifts in band positions caused by elemental substitutions. Because the thermospectrum for each mineral is unique, it is a useful quantitative measure for determining pyroxene compositions in remote sensing data acquired at a range of temperatures. Further work will involve evaluating these minerals across the visible wavelength range and deriving a function that provides a model for a variety of compositions at a range of surface temperatures found across the Solar System.

References: [1] Schade U. and R. Wasch (1999) *Adv. Space Res., 23,* 1253–1256. [2] Singer R. B. and T. L. Roush (1985) *JGR, 90,* 12,434-12,444. [3] Roush T. L. and R. B. Singer (1986) *JGR, 91,* 10,301-10,308. [4] Hazen R. M. et al. (1978) *LPSC IX,* p. 2919-2934. [5] Cloutis E. A. (2002) *JGR, 107,* 6-1 to 6-12. [6] Klima R. L. et al. (2007) *Meteoritics & Planet. Sci., 42,* 235-253. [7] Klima R. L. et al. (2011) *Meteoritics & Planet. Sci., 46,* 379-395. [8] Hinrichs J. L. and P. G. Lucey (2002) *Icarus, 155,* 181-188.

Acknowledgements: This work was supported in part by an appointment at the JHUAPL administered by ORISE through an interagency agreement between the U.S. Department of Energy and APL.